ICES Journal of Marine Science, 57: 1204–1217. 2000
doi:10.1006/jmsc.2000.0806, available online at http://www.idealibrary.com on IDEAL®

Measurement and removal of echo integration noise

Rolf J. Korneliussen

Korneliussen, R. J. 2000. Measurement and removal of echo integration noise. – ICES Journal of Marine Science, 57: 1204–1217.

Pushing scientific echo sounders to the limit involves the consideration of "noise", which is inherently frequency dependent and which also depends on bottom depth. Here, noise is quantified by measurement with a standard echo sounder, the SIMRAD EK500, at 18, 38, 120 and 200 kHz. The use of empirical relationships of noise as a function of range to reduce echo integration is described in general, and illustrated in particular, for data collected on the stock of Norwegian spring spawning herring (*Clupea harengus*) when wintering in the Vestfjord system.

Key words: acoustic noise, acoustic survey, echo integration, bottom reverberation, echo integration noise.

Received 13 April 1995; accepted 9 May 2000.

R. J. Korneliussen: Institute of Marine Research, P.O. Box 1870 Nordnes, N-5817 Bergen, Norway. Tel. +47 55 23 85 00 (6853); fax: +47 55 23 85 84; e-mail: rolf@imr.no.

Introduction

Echo integration based on a single frequency is commonly used to estimate fish stock abundance (MacLennan, 1990). The frequency of 38 kHz often adopted is a compromise between the need for detection ranges of the order of hundreds of metres and need to detect single fish and small animals. For very small animals, e.g. zooplankton, higher frequencies are needed at the cost of shorter range. For improved classification and abundance estimation of animals, a multi-frequency system can be used. This can also be used to some extent to investigate the tilt angle of detected fish.

With respect to extracting more information from multi-frequency systes, the data should be comparable between frequencies, ping-by-ping, at all depths. The transducers should be positioned as close as possible and have identical half power beamwidths (one way). Sound transmission should be simultaneous and the pulse duration should be the same for all frequencies. All systems should be calibrated; noise has to be reduced to a negligible level. All but one of these conditions may be met – by using proper settings on the echo sounders: "noise" is the exception, especially so for high frequencies.

On R/V "Johan Hjort" the frequencies 18, 38, 120, and 200 kHz are available on the echo sounder SIMRAD EK500. Noise is an increasing problem at 120 kHz beyond 150 m range from the transducer, even for optimal settings of the echo sounder (SIMRAD, 1997), and a serious problem beyond 200 m. At 200 kHz, problems begin at even shorter ranges. In Norwegian waters large concentrations of herring (*Clupea harengus*) are located between 200 and 300 m depth (Huse and Korneliussen, 1993), making noise removal necessary at least for 120 and 200 kHz. After noise removal, the effective range is limited by the acoustical sampling volume (Aglen, 1982; Ona, 1987; Foote, 1991).

The most obvious way of removing noise is to use the noise-reduction function incorporated in the EK500. For each ping the echo sounder samples the received power, and uses the median value to represent noise, but it is questionable if and when this median value actually represents noise. The measured value will obviously be greater than the noise for very large and dense concentrations of fish or plankton. Even at lower concentrations the technique will give incorrect results, since the measurements are only "thresholded" and not corrected, meaning that a sample is either set to zero or used as it is. There is no attempt to correct a measured value. As a result of the improper noise reduction function in EK500, noise has to be removed by post-processing techniques.

The problem of noise reduction is not new: Nunnalee (1987) described a theoretical technique in which noise was estimated from data collected with the echo sounder

operated in passive mode i.e. no sound transmission. Thus, noise was determined from data periodically collected other than when density measurements themselves were taken. The calculated noise is not necessarily applicable to the data used in abundance estimation, especially in the presence of rapid noise variations.

As did Nunnallee (1987), Takao and Furusawa (1995) estimated noise from passive data. Data were collected with a transducer mounted on a towed body, so that the measured noise was dependent on the position of the towed body relative to the ship. Noise was reduced by thresholding data, which gives incorrect results except for strong targets where the bias is negligible.

Watkins and Brierly (1996) found the minimum volume backscattering coefficient s_v for each depth and used this to calculate noise, or ''offset'' as they called it. The advantage of this method is that it uses data from ordinary survey operations. Watkins and Brierly claim to be able to monitor noise within a given time period but this has not been demonstrated; they do not state whether they found a representative value for the noise.

None of the studies mentioned above discuss the physics of the potential noise sources nor how rapidly and how much noise can change with the surroundings. This is particular a weakness of the work by Nunnalee (1987) and Takao and Furusawa (1995), since data for noise calculation is collected separately from the other data. In general, wind or sea-generated noise is expected to dominate below 10–20 kHz according to the Knudsen spectra (Medwin and Clay, 1998; Urick, 1983) and thermal or instrument noise above 200 kHz. Own-ship noise and possibly biological noise can also be important. Frequencies of interest in fisheries acoustics are in the range 12 to 200 kHz, so all of the indicated noise sources can be important. A new method to calculate noise from survey data is desirable.

The purpose of this study is to derive and illustrate a practical technique to quantify and remove noise from echograms. The physical processes are not considered but noise is separated into varying noise, and persistent noise, which probably arises from instruments. Noise dependence on weather is not a topic for this study even though some measurements were performed in bad weather. A good description of the wind dependence of noise is given by Hall (1989).

Theory

Model

A proper definition of noise is needed before developing a model to remove it. In general, noise is all unwanted signals, including transmitted sound backscattered from wind-generated bubbles. It is, however, difficult to separate free bubbles from swimbladders in small fish, or bubbles generated for buoyancy by some types of plankton. If the desired signal is defined as all transmitted sound backscattered on to the transducer surface, then noise is everything else. Sound generated by ships, animals, collapsing bubbles, wind or sea is defined to be noise in this case, as is instrument noise not associated with the transmission of sound. With this definition, backscattered sound caused by unwanted electrical signals in the transmit part of the echo sounder is not regarded as noise, and neither is sound backscattered from bubbles.

The noise and signal propagation in the system is shown in Figure 1. Acoustic transducers convert the received acoustic pressure to voltage. The voltage is squared by the software to make it proportional to power. Noise is added from each of the separate parts of the echo sounder system: the transmit electronics, the transducer, unwanted sources in the medium, and the receiving electronics. It propagates all the way through the system. Noise generated by external electronic devices may also be picked up by the echo sounder and cables. Noise can also be introduced by limited numerical resolution or a low sampling frequency, combined with inappropriate signal processing. The noise picked up by the receiver system is squared, together with the signal backscattered from objects in the insonified volume. After range compensation (MacLennan, 1990) and adjustment by calibration factors, the measured data are available at absolute levels.

The mean volume backscattering coefficient can be expressed as:

$$s_V = C^2 \mathrm{Ave}[g(t)(U_S + U_N)^2] \quad (1)$$

where C is then a constant including all calibration factors, also beam directivity expressed through the transducers equivalent beam angle Ave(x) is the sample mean of x. The time varied gain g(t) compensates for range, U_S is the signal and U_N is the noise part of the measured signal. Equation (1) can be separated into two terms:

$$s_V = s_V = s_{V,S} + S_{V,N}, \quad (2)$$

where $s_{V,S}$ is the sought signal and $s_{V,N}$ is the noise. Note that $\mathrm{Ave}(U_S U_N) = 0$ is assumed, i.e. noise and signal are uncorrelated.

Each available $s_{V,N}$ is averaged from m samples internally in EK500: $s_{V,N} = (C^2/m)\Sigma_{i=1}^{m} g(t_i) U_{N,i}^2$. For a short depth interval, this approximates well to:

$$s_{V,N} = C^2 g(t) \mathrm{Ave}(U_N^2). \quad (3)$$

Introducing the noise power index N:

$$N \equiv s_{V,N}/g(t), \quad (4)$$

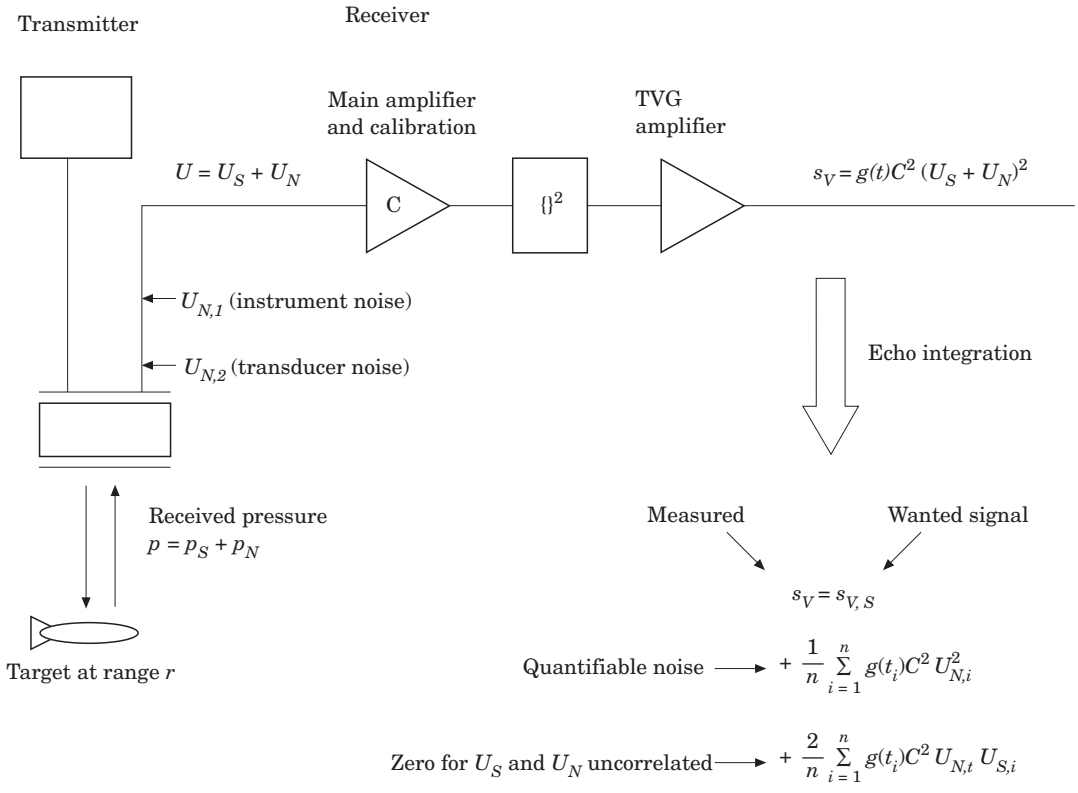

Figure 1. Signal and noise propagation in the system. The variables with index S represent wanted signal and the variables with index N represent noise. Instrument and transducer noise are placed on the receiver side for convenience.

the new noise correction algorithm can be expressed as follows:

$$s_{V,S} = \begin{cases} s_V - g(t)\mathrm{Ave}(N) & \text{if } s_V \geq g(t)N_H \\ 0 & \text{if } s_V < g(t)N_H, \end{cases} \quad (5)$$

where N_H is the upper limit of the noise power index. The averaging in equation (5) is based on the available values of $s_{V,N}$, which are calculated from m samples internally to the echo sounder as stated above.

The noise power index N is preferred to the received power for noise calculations, since echo sounder systems are calibrated with respect to the volume backscattering coefficient s_V.

Realization: measurement principles

Pure noise $s_{V,N}$ is only available from data collected with the echo sounder in passive mode, where $s_V = s_{V,N}$. For the echo sounder operated in active mode, the noise power index N must be estimated from the measured volume backscattering coefficient $s_V = s_{V,S} + s_{V,N}$, when signal and noise coexist.

Often there are no interesting or significant scatterers in the water column so the most frequent measurements then are of noise only. However, this is not true in dense concentrations of plankton and fish, and therefore measurements of active sound cannot generally be used directly to estimate noise. The only difference, however, between the echo sounder operated in passive mode and in the receiving phase of the active mode is the backscattering of the transmitted sound. In active mode the echo sounder transmits a sound burst that lasts for a few milliseconds before it switches to receiving mode. The bottom is the last scatterer in the water column. Consequently, when the bottom echo has disappeared the recorded data are purely passive and are therefore suitable for estimation of noise by Ave(N) and N_H. The time it takes for the botto echo to disappear is estimated from experimental data. The question is whether the bottom echo from the first direct path has vanished before multiple echoes, e.g. from bottom–surface–bottom, are received.

For standard software versions of EK500 the sampling distance for internal data processing is frequency dependent (see Table 1 or SIMRAD, 1990–1997), but usually only the mean values of s_V are accessible for post-processing. For the 38 kHz data collected with 1 m vertical resolution, each value of s_V is a mean of 10 samples. This averaging is not a problem as long as s_V

Table 1. Echo sounder settings and transducers used.

		EK500–1		EK500–2
Noise margin		0		0
Frequency (kHz)	18	38	120	200
Transducer (SIMRAD)	ES18-11	ES38B	ES120-7	200-28
3 dB beam width (deg.)	11.0	6.9	7.1	7.0
2-way beam angle (dB)	− 17.1	− 21.0	− 20.6	− 20.4
Peak transmit power (W)	2000	2000	1000	1000
Pulse duration (ms)	0.7 (Short)	1.0 (Medium)	1.0 (Long)	0.6 (Long)
Bandwidth (kHz)	1.8 (Wide)	3.8 (Wide)	1.2 (Narrow)	2.0 (Narrow)
2-way beam angle (dB)	− 17.1	− 21.0	− 20.6	− 20.4
Sampling distance (cm)	25	10	3	2
Number of samples per m	4	10	33.33	50

are computed from noise samples only, as is the case for samples measured after the vanished bottom echoes. The only effect of the averaging would be to reduce the variance around Ave(N), that is to reduce the value of N_H.

In the active mode $N=s_{V,N}/g(t)$ in equation (5) is substituted by $s_V/g(t)$ and Ave(N) by N_E, since pure noise is not available, as the definition of N demands. An upper value which is less than infinity has to be found for N_H. Based on the experimental recorded probability density function f, N_T used to define $N_{H,10}$ below is expressed through the maximum of f, that is $f(N_T)=MAX\{f(s_V/g(t))\}$. $N_{H,10}$ is the value of N_H corresponding to $f(s_V/g(t))$ equal to 10% of f at maximum, that is 10% of $f(N_T)$ as expressed in equation (6):

$$N_{H,10}=s_V/g(t) \text{ where } f(N_{H,10})=f(N_T)10^{-1} \text{ and } N_{H,10}>N_T. \quad (6)$$

Ave(N) is now substituted by:

$$N_E=\text{Ave}(s_V/g(t)) \text{ where } s_V/g(t)<N_{H,10} \quad (7)$$

The alternative expression of equation (5) for active pinging when $s_{V,N}$ is not available is:

$$s_{V,S}=\begin{cases} s_V-g(t)N_E & \text{if } s_V\geq g(t)N_{H,10} \\ 0 & \text{if } s_V<g(t)N_{H,10} \end{cases}. \quad (8)$$

Furthermore it should be understood that N_E and $N_{H,10}$ are used in combination with active data to estimate Ave(N). The expressions Ave(N) and N_H are only used in combination with data recorded in passive mode. In this case all measured data are noise, so there is no need to set an upper limit for N_H to calculate Ave(N).

Establishing histograms of $s_V/g(t)$ can be difficult in situations with rapid and large variations of noise. The number of measurements used in each histogram depends on how often noise is computed, that is if noise should be computed from one ping only or if it should be an average over thousands of pings. Use of a standard width for the histogram cells and standard upper and lower limits for the histograms will sometimes impede the computation of a stable and accurate value for low noise and sometimes make it impossible to calculate high noise because of limited memory in the computers used. The problem can be solved by increasing the cell width linearly or nonlinearly with increasing noise level. Another solution is to calculate the cell limits and the upper and lower limits of the histogram dynamically and this is the solution used here.

The algorithm is the following:

(1) An approximate value of median $s_V/g(t)$ is found for each echogram. On average, an echogram contains 10^6 s_V values. Values closer than 5 m from the transducer are not used in any calculation due to transmission pulse, near-field effects and effects of radiation from the backside of the transducer into the ship hull plates.

(2) Based on the median, the upper and lower limits of e.g. a 2000-cell histogram are calculated for each echogram. Alternatively, standard histogram limits can be used for all echograms to speed up the calculations if the noise is known not to vary much. The number of histogram cells can be changed.

(3) Histograms are calculated for a given distance, e.g. 0.05 nautical miles, and N_E (or Ave(N)) and $N_{H,10}$ are calculated and stored together with sailed distance, time and other variables. If there are fewer than a given number of the $s_V/g(t)$ data for the given distance, the distance is automatically increased before N_E and $N_{H,10}$ are calculated.

(4) In addition to calculating the same variables for the total echograms as for the echogram-segments under (3), the histograms used in the calculations are stored as depth channels parallel to the surface and to the bottom, respectively, and as a histogram based on the total echogram. At the Institute of Marine Research the echograms are standardized to contain five nautical miles of data.

Experimental data can indicate how many data samples are needed to calculate Ave(N) and N_H.

The assumption of uncorrelated signal and noise

The theory postulated is valid provided signal and noise are uncorrelated, which in combination with averaging or summing a large number of samples removes the combined signal and noise part of s_V. This assumption is explored before designing the experiments: The most likely noise sources are instrument, propeller and sea-generated noise. The propeller and sea-generated noises should be uncorrelated with scattering from fish. The instrument noise is also expected to be uncorrelated with the signal, even if it is temperature dependent. The power amplifiers inside the EK500 generate heat, but the instrument temperature is not expected to change significantly from active to passive operation of the transducer. In general, signal and noise are uncorrelated, and consequently the method proposed is valid.

Each of the area backscattering coefficients s_A to be stored is calculated from s_V samples by summing in the direction of depth and averaging in the direction of motion. The relation between the stored s_A and the internal samples $s_{V,i}$ in EK500 is given by: $s_A = (\Delta r/l)\Sigma_{i=1}^{nl} s_{V,i}$, where Δr is sampling distance, l is number of pings, and n is number of vertical samples. As an example, a distance of 0.1 nautical miles containing $l = 20$ pings stored with a $\Delta z = 10$ m channel thickness for 18 kHz can be assumed. Each stored s_A is then based on nl samples where $l = 20$ and $n = \text{round}(\Delta z/\Delta r) = \text{round}(10/0.25) = 40$, thus $nl = 800$. Hence the number of samples used to calculate s_A values with this fine resolution to be stored in the database is large enough to use the technique.

Materials and methods

Equipment and pre-processing software

Data were collected from R/V "Johan Hjort" using a SIMRAD EK500 V5.30 or 5.20, and stored in files by means of the Bergen Echo Integrator system (BEI) (Foote *et al.*, 1991; Korneliussen, 1993). Two EK500 echo sounders were used in parallel to control four transducers. The transducers at 18, 38 and 120 kHz were split-beam devices mounted on a protruding keel and controlled from the same EK500, called EK500_1. The protruding keel could be locked in any position from 0–3 m below the bottom of the ship hull, which has a depth of about 5.0 m below the sea surface. The protruding keel was used to lower the transducers below the bubble concentrations and thereby reduce the backscattering from bubbles (Ona and Traynor, 1990). The single-beam 200 kHz transducer was hull mounted at about 5.5 m depth and was controlled from the second EK500, called EK500_2. All transducers were piezoelectric and highly directional with a 3 dB opening angle of about 7° for the 38, 120, and 200 kHz transducers and about 11° for the 18 kHz transducer (see Table 1). The sampling distances for standard versions of EK500 are fixed to the values shown in Table 1 and cannot be changed. The transmit power of the transducers was 2 kW at 18 and 38 kHz and 1 kW for 120 and 200-kHz for all measurement series. The pulse lengths were selected as close to 1.0 ms as possible with the multi frequency echograms in mind. The bandwidths were selected to minimize noise, but in accordance with recommendations of the EK500 manual. The two EK500 systems were calibrated with their transducers and with the settings in Table 1 according to Foote (1982) and Foote *et al.* (1987).

Experimental design and data collection

The data were collected in five series E1–E5. In experiments E1 and E2 instrument noise and interference between frequencies was studied. These provide references for very low noise conditions. In experiment E3 special effects caused by the placement of the transducers on the protruding keel were studied *vis-à-vis* the propeller. Particular aspects of the method were tested in experiments E4 and E5: E4 for its ability to quantify rapid and sometimes large changes of noise, and E5 for the validation of data received after the bottom echo to calculate noise. Experiment E4 also served as an investigation of the importance of propeller noise backscattered from the bottom. A collection of the experimental objects of noise investigation is given in Table 2 in five measurement series.

The noise margin was equal to zero for the collection of all data, which means that the EK500 did not remove noise by internal algorithm. Note that the EK500_2 was triggered from EK500_1 which gave a few milliseconds time-delay in the sound transmitting from the EK500/200-kHz system as compared to the others.

Data for experiments E1–E4 were collected with EK500 V5.30 between 22 November 1997 and 14 January 1998 in the Vestfjord–Ofotfjord waters in northern Norway, with low plankton concentrations. Data for experiment E5 were recorded in the Barents Sea at 7 September 1997 with EK500 V5.20.

Experiment E1

Data for E1 were collected with the ship drifting at position (68°29′N, 17°25′E) in Ofotfjorden. The sea-state was 0–1, with essentially no wind, activities on deck were suspended and the propeller was not rotating but the main machinery was not stopped. The location was shielded by mountains with steep shore slopes making little wind, which reduces the amount of bubbles in the water. The bottom depth was about 110 m, and the

Table 2. Experimental objects of noise investigation in five measurement series.

	Persistent noise		External noise		Validation
	E1: Minimum noise	E2: Interference between freq.	E3: Keel depth dependence	E4: Bottom dependence	E5: Noise-extraction during active pinging
Active/passive	P	P, one active	P	P[a]	P/A
Result in figures	2	3	4	5	6
Vessel speed (knots)	0	0	11	11	11
Bottom depth (m)	110	110	+2500	50–550	450
Keel depth (m)	1.0	1.0	0.0–3.0	2.0	2.0
Sea state (Beaufort)	0–1	0–1	2	1–2	1–2
Wind speed (knots)	<2	<2	4–9	4–9	4–9

[a]120 kHz active to get bottom depth.

water temperature was typically between 5.5 and 7.5°C throughout the water column. In E1, both echo sounders were operated in passive mode and the data were recorded simultaneously at all frequencies.

Experiment E2

Data collection for E2 followed immediately after the recordings for E1 with some data in common. The passive operation for all frequencies was followed by passive operation for all except one frequency that was active at a time.

Experiment E3

Data for E3 were collected outside Vestfjorden along the line (69°N, 12°E)–(70°N,9°30′E). The bottom depths were more than 2500 m, the sea state was 2, the wind speed was 4–9 knots and the propeller rotated at 125 rpm, resulting in the most common cruising speed of somewhat more than 11 knots. The protruding keel was moved in the following sequence: 2.0–3.0–2.5–1.5–1.0–0.5–0.0–2.0 m, where the numbers are given in metres out of the ship hull. The data were recorded with the echo sounder operated in passive mode. The bottom depths were measured occasionally with the echo sounders operated in active mode at the same time as CTD data were measured. The water temperatures decreased from above 7°C at 20 m depth to 0.65°C at 1500 m depth.

Experiment E4

Data for E4 were collected in Ofotfjorden with the EK500 operated in passive mode at 18, 38 and 200 kHz while the ship was cruising in the middle of the fjord far from the steep shore slopes. Bottom depths were measured with the EK500/120-kHz system in active mode with all frequencies triggered simultaneously. As in E1 and E2, the fjord was surrounded by mountains 500–800 m high, reducing the potential problems of backscattering and active generation of sound from bubbles because they minimize both the wind and waves needed to generate bubbles. The protruding keel was 2 m out of the hull, and which also produces the same effect.

Experiment E5

Data for E5 were collected in a typical fish abundance survey in the Barents Sea during calm weather conditions, with little wind and waves to avoid weather-generated noise. Data were collected at all four frequencies, first in passive mode for comparison, then with the active transmitting of sound.

At least two measurement series for each of E1–E5 were done for comparison but only one of each is presented here. In addition to E1–E5, some data were collected to look for noise-effects at stronger wind speeds (30 knots).

Results and discussion

The experiments are separated into three groups: persistent noise, external noise and validation of the noise extraction method during active pinging. The results from one group of experiments bear on the conclusion to be drawn from the next. Experiment group I contains the experiments E1 and E2, group II contains E3 and E4, and group III contains E5.

Low noise experiments: persistent noise experiments E1 and E2

The experimental probability density function f(N) from experiment E1 is shown in Figure 2. The noise is expected to be close to the lowest possible for the equipment used when the ship is cruising. The weather did not generate noise because of the exceptionally calm conditions. The potential noise sources were the machinery, instrument noise, thermal noise and possibly other types of external noise. f(N) showed no depth dependence, and therefore all data from the echograms were used to generate Figure 2a–d. Ave(N) and $N_H = N_{H,10}$ are marked in Figure 2a.

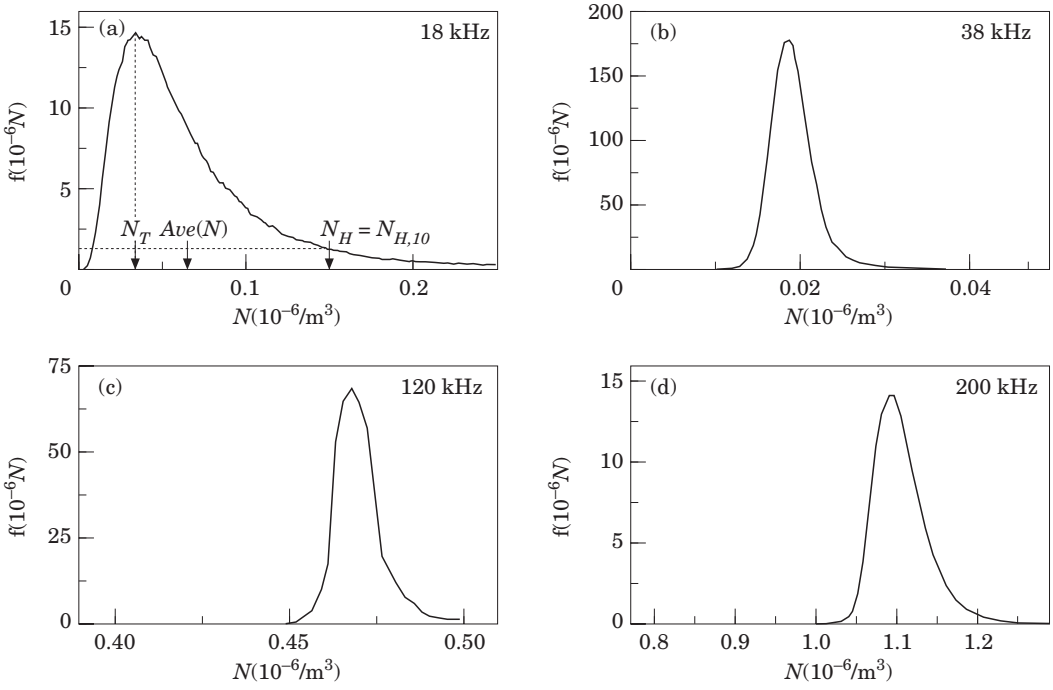

Figure 2. Experimental probability density function f of the noise power index N ($\times 10^{-6}$/m^3) for 18–200 kHz under the presumed lowest possible noise conditions. The weather was very calm, the ship was not moving, the main engine was not running and all deck activities were suspended. The data were recorded with 1 m vertical resolution and the echo sounders were operated in passive mode. For 1 m resolution, each available s_V is the mean of four samples for 18 kHz data, 10 for 38 kHz data, 33–34 for 120 kHz data and 50 for 200 kHz data (see Table 1). The same data are shown as time varying noise in Figure 3 from 0–1850 sec.

The s_V measurements used to generate Figure 2 were collected by setting the EK500 depth range to 500 m. As noted earlier, each s_V value is a mean of several samples dependent on both frequency and set range. This reduces the variance as compared to measurements where the range is set to give only one sample per s_V. Figure 2c (120 kHz) and d (200 kHz) both show large offsets to the first non-zero s_V, and the offsets are confirmed from measurements with only one sample per s_V value. The offsets found for 120 and 200 kHz varied little during a single measurement series as shown in Figure 3, but also varied little between several experiments at low noise conditions. The stable offsets in the different measurement series indicates low interference with other electronic equipment onboard the ship, at least if the electronic equipment is not continuously used. The most likely persistent noise sources are therefore instrument noise and thermal noise.

The offset for 38 kHz data with 10 samples per s_V value in Figure 2b is small, and is further reduced to less than the half of this value in the measurement series with only one sample per s_V. For 18 kHz data, the offset can be ignored. Thus for the EK500/18-kHz and the EK500/38-kHz systems, the instrument noise can be ignored as compared to EK500/120 and 200 kHz systems.

For further investigations of the instrument noise, the width of the "noise peak" ΔN_T is introduced as the difference between the N values 3 dB down from the top $f(N_T)$. The noise variability $N_T/\Delta N_T$ increases with the number of samples used by EK500 to calculate each s_V value. Since thermal noise is expected to increase with frequency, and since the number of samples per s_V for 200 kHz is larger than for 120 kHz it is surprising that one finds a larger value of $N_T/\Delta N_T$ at 120 kHz as shown in Table 3. The only possible explanation of this is strong instrument noise within the EK500/120-kHz system.

The 18 kHz noise distribution in Figure 2a differs by a larger "tail" as compared to the other distributions. If instrument noise is ignored for the EK500/18 kHz system the received power is proportional to $(U_N)^2$ and N. It can easily be shown that a normal distributed noise p_N in the received pressure p would be detected as a Rayleigh distribution in received power due to the envelope detection used by EK500. However, the tail in Figure 2a has a significantly larger tail area than in a Rayleigh distribution. A part of the tail can be explained by the existence of several external noise sources. The tail cannot be caused by the EK500 hardware or by the software: the numerical resolution in the EK500 data will "discretize" the stored s_V values, but the average of

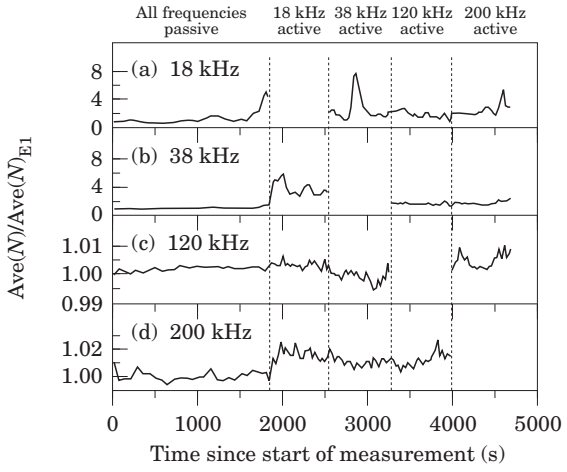

Figure 3. Noise influence between frequencies. The transducers are active one by one in the following sequence: non, 18 kHz, 38 kHz, 120 kHz, 200 kHz with switches at about 1850, 2550, 3260 and 3980 sec from the start. The mean noise power index Ave(N) is normalized to its value $Ave(N)_{E1}$ between times 0–1850 sec from start where it was no transmitting of sound. These data are also used in experiment E1 shown in Figure 2.

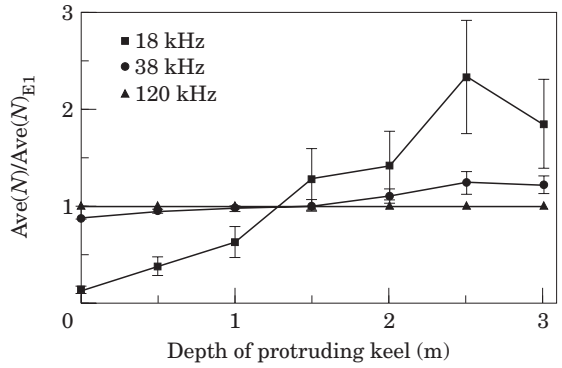

Figure 4. Noise dependence of the depth of the protruding keel at calm weather conditions with ship cruising at 11 knots. The bottom depths are very deep. For each frequency, the mean noise power index Ave(N) is normalized to $Ave(N)_{E1}$ with the protruding keel 2 m out of the hull. The measurements of $Ave(N)_{E1}$ were done especially for this experiment. The uncertainties are based on the two measurements series with the keel 2 m out of the hull, and are displayed at the other depths with the same percentage uncertainty. The measurement uncertainties for the 120 kHz data are too small to be shown. The depth uncertainties of the depth of the protruding keel was about 10 cm.

Table 3. Noise variability.

Frequency (kHz)	18	38	120	200
$N_T/\Delta N_T$	0.6	3.5	40	17
Samples per s_V	4	10	33.33	50

this rounding error is close to zero. For reasonably wide histogram cells, the effect of discretizing will disappear. For narrow histogram cells the approximation in equation (3) has a slightly smoothing effect on the discretizing, but not as much for the 18 kHz as for the other frequencies because of the fewer samples used to compute each stored s_V value. In total the stretched tail for the 18 kHz histograms, as compared to the other histograms, is an indication of the greater importance of external noise at the EK500/18 kHz systems. This is hardly a surprise but the result of experiment E1 allows further investigation of noise as measured on board R/V "Johan Hjort" by EK500 connected to the available transducers.

Values of normalized average noise power index $Ave(N)/Ave(N)_{E1}$ from experiment E2 is shown in Figure 3. The subscript E1 is used, since the same data were used in experiment E1 shown in Figure 2. The transducers were activated in the following sequence: none, 18 kHz, 38 kHz, 38 kHz, 120 kHz, 200 kHz, with switches at about 1850, 2550, 3260 and 3980 sec from the start as indicated in Figure 3. The 18 kHz noise in Figure 3a varies greatly but there is no clear dependency between measured noise and active pinging from 38, 120 or 200 kHz. The two peaks shown at about 1800 and 2800 sec from the start are only seen in Figure 3a for 18 kHz. It is unclear if own ship is the origin of these noise peaks, e.g. by coupling in the propeller for a few seconds to keep the position, but is important that none of the other frequencies seem to be affected. At 38 kHz, noise increased by about 300% when 18 kHz was active and by about 50% when either 120 or 200 kHz was active. However, even with 300% increase in average noise 38 kHz was less noisy than the other frequencies. The 120 kHz system seems to be interfered with by the other frequencies but there is no significant increase in noise. The 200 kHz system has a small but significant increase in noise when any of the other frequencies are active. Since the noise at both 38 and 200 kHz increases slightly for active transmitting of sound at any of the other frequencies, it is surprising that the 120 kHz noise measurements do not increase. It seems likely that the interference from the other frequencies becomes insignificant compared to strong instrument noise at 120 kHz.

The main result of the experiment is to show that active pinging at any of the four frequencies interferes with the others for the EK500 settings and transducers used, but the additional noise caused by active pinging can be ignored except for the EK500/38 kHz system.

External noise experiments E3 and E4

Noise dependence on transducer depth, E3

Average normalized noise at 18, 38 and 120 kHz in calm weather at standard cruising speed is shown in Figure 4

as a function of transducer depth. The data for E3 were collected prior to removal and re-inserting of the EK500 V5.30 PROM set, so the noise is normalized to a separate set of values from an experiment of type E1 with the keel 2 m out of the hull. The values of $Ave(N)_{E1}$ this experiment E1 as compared to the measurements shown in Figure 2 were 0.97 for 18 kHz, 0.46 for 38 kHz and 0.98 for 120 kHz. The calm weather in experiment E3 reduced the problem of bubble-scattered propeller noise compared to bad weather. The number of bubbles decreased with depth and therefore bubble-backscattered propeller noise should also decrease with depth. The uncertainties are based on the two repeated measurement series at 2 m keel depth.

The normalized noise with the keel 2 m out of the hull was expected to be greater than 1.0 at all frequecies because of the additional propeller and flow-noise when the ship was cruising, but Figure 4 shows that the additional noise measured is barely significant. The recorded average noise index does not change much with varying keel depth at 120 and 38 kHz transducers. At 18 kHz, however, a significant increase in average noise power index is seen with increasing keel depth. Although the reasons for this are rather unclear, it seems likely that the structural vibrations of the hull generated from the main engine, auxillary generator and gearbox may be picked by the EK500/18 kHz system. With the keel retracted, the ship's hull shadows the keel-mounted transducers from the propeller's direct radiation. The radiation pattern for the 18 kHz transducer is much wider than for the others and some of the minor sidelobes may pick up direct radiation from the propeller. However, if the propeller caused the observed effect the noise should be greater at all keel depths than the average noise in experiment E1, when the propeller was not rotating at all. Noise from weather-generated collapsing bubbles is probably less noisy than the propeller. One remaining possibility is vibrations of ship machinery coupled in some way to the ship's hull and the protruding keel. Vibrations in the protruding keel probably increases with keel depth.

Note that the data are recorded in calm weather with EK500 operated in passive mode, and that the noise dependence of the keel depth might differ in bad weather. For active transmission of sound, for example, the bubble clouds are surely a problem, even if backscattered sound from bubbles is not covered by the definition of noise here.

In summary, the experiment shows that the depth of the protruding keel is of importance for the measured noise, especially at 18 kHz, but no prediction is made on how the keel depth influences the noise. The conclusion is that noise removal according to the equations (5) and (8) requires that both noise and the acoustic signal have to be recorded with the keel at the same depth.

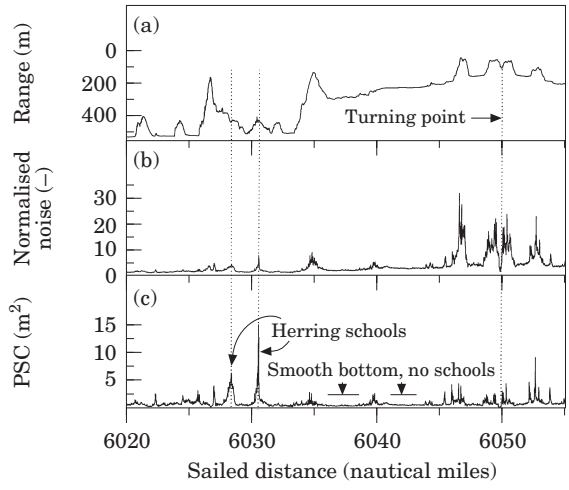

Figure 5. Bistatic range (a), square root of normalized noise $(Ave(N)/Ave(N)_{E1})^{1/2}$ (b) and calculated propeller source coefficient $PSC=g(t)Y/10^6$ (c) plotted against sailed distance. Y is the normalized varying noise, i.e. compensated for persistent noise $Y=[(Ave(N)-Ave(N)_{E1})/Ave(N)_{E1}]$. The persistent noise $Ave(N)_{E1}$ cannot be caused by the propeller and is therefore subtracted from Ave(N). The result is multiplied with the range compensating function g(t) to remove the effect of the bottom. $t=r/c$ is the sound travel time propeller-bottom-transducer where c is the speed of sound and r is the bistatic range in (a). If the propeller is the dominating and a stable noise source, if the bottom is smooth with the same sediment type for all data and if there are no scatterers in the water column the result PSC should result in an almost straight line in (c).

E3 is gruped together with E4 as external noise, but it might also be grouped with the persistent noise experiments. The result is a keel depth-dependent persistent noise.

Noise dependence on bottom depth, E4

The result of experiment E4 for 18 kHz is shown in Figure 5a–c. The data were collected with the depth range of EK500 set to 1000 m, i.e. eight samples per s_V value, and were averaged over 0.01 nautical miles, which is about 16 sec of data at 11 knots or typically about two pings. Bottom depth was found by using the 120 kHz transducer in active mode. This active pinging did not disturb the noise measurements according to the results of experiment E2. The process of noise quantification from an echogram containing 10^6 measurements can be done in a few seconds routinely, even with the need to calculate ping-to-ping variations in noise.

The upper curve, Figure 5a, is the bistatic range which is half the distance "propeller-bottom transducer". The middle curve, Figure 5b, is the mean noise power index Ave(N) at 18 kHz, visualized as the square root of measured mean normalized noise: $(Ave(N)/Ave(N)_{E1})^{1/2}$. These two curves show that noise can be predicted from the bistatic range, with some exceptions.

Figure 5c shows the result of a simple model trying to calculate a number proportional to radiated power from the propeller, provided that the propeller is the only noise source. This simple model also provides that the roughness and hardness of the bottom do not vary, and that the bottom slope is small. Normalized varying noise is introduced as:

$$Y \equiv [\mathrm{Ave(N)} - \mathrm{Ave(N)_{E1}}]/\mathrm{Ave(N)_{E1}}. \quad (9)$$

$\mathrm{Ave(N)} - \mathrm{Ave(N)_{E1}}$ is varying noise, i.e. measured noise compensated for persistent noise found in experiment E1. The denominator $\mathrm{Ave(N)_{E1}}$ is used to make the numbers dimensionless.

The new term ''propeller source coefficient'' (PSC) is expressed as:

$$\mathrm{PSC} \equiv g(t)Y/10^6. \quad (10)$$

The factor g(t) compensates for the distance ''propeller-bottom-transducer''. The denominator 10^6 is used to make the numbers smaller and therefore easier to read. PSC for 18 kHz is shown in Figure 5c.

Several schools located at 50–75 m depth are found on the 120 kHz echogram up to distance sailed of 6031.5 nmi. The two high peaks marked in Figure 5c are both identified as schools. The density of the first school in the zone 6027.2–6028.8 nmi fits nicely, except for the height of the leading peak, from the image of the echogram with the densest part of the school at the end. The second school marked in Figure 5c is found between 6030.0–6031.4 nmi in the echograms, but this school is not as dense as the first. The higher peak for the second school may indicate that the ship did not pass over the centre of the school. We recall that the 18 kHz transducer has a 11° half power beamwidth compared to the 7° of all the other transducers. Inspection of the same peak in figures similar to Figure 5c at 38 kHz supports this hypothesis.

The ship turns at 6049.7 nmi so that the cruise lines from 6045.0–6050.0 nmi and 6050.0–6055.0 nmi are about the same length but run in opposite directions. The increased noise found between 6045 and 6055 nmi compared with the model is not explained by schools but by the proximity of the bottom and the reduced geometrical loss of propeller noise. Multiple reflections (propeller–bottom–ship/surface–bottom–transducer) reduce the geometrical loss at shallow depths. Inspection of the depth conditions shows that bottom variations, both with respect to orientation and hardness, can explain some of the fluctuations. The most shallow locations are often covered by less mud than the deeper locations. Plotting the derivative of the bottom depth against noise did not give a clear enough picture to be presented here. Only 18 kHz record is shown here, but data from 38 kHz shows the same picture.

No biological samples for clams or shrimps were taken at the shallow locations between distances 6045–6055 nmi because of difficult conditions for biological sampling. However there were no indications of shrimps in the active 120 kHz echograms. Further, based on discussion with biologists, there are no species of snapping shrimps or clams capable of making significant noise at this location and depth.

The sections 6036–6038.5 nmi, 6041–6044 nmi and also that from 6047.2–6048.3 nmi have a smooth bottom with no schools visible on the 120 kHz echograms. The computed values of PSC at 18 kHz are about the same value for all three distances, and this supports the hypothesis of bottom reflected propeller noise as one of the main noise sources. An equally important conclusion from this experiment is that it is possible to compute rapidly changing noise with the noise extraction method used. Measurement of R/V ''Johan Hjort'' 's vessel noise by external hydrophones show a low frequency noise level of about 150 dB re 1 μPa/$(\mathrm{Hz})^{1/2}$ at 1 m in the frequency region 10–400 kHz, falling by about 20 dB per decade. The noise level at 125 RPM, 74% pitch giving 12.1 knots were measured 29 November 1990. Details of underwater noise from various studies are given in Mitson (1995).

Wind and sea-generated noise and backscattering from bubble clouds

No systemic investigation of bad weather noise was performed because this was irrelevant to the proposed approach and much work has been carried out in this field already, e.g. Hall (1989).

An impression of the influence of bubbles in bad weather can be seen from backscattered propeller noise caused by herring schools. Since herring have air-filled swimbladders, its schools could be regarded as bubble clouds composed of very large bubbles. One measurement series was done in a 28 knot wind with the keel mounted transducers 3 m below the hull at 8 m depth below the sea surface. EK500 was operated in passive mode. There was, surprisingly, no measurable effect on neither 18 kHz, 38 kHz nor 120 kHz. There were visible effects *via* the active transmission of sound from the hull-mounted 200 kHz transducer but only a minor measurable effect with passive recordings. Active use of the protruding keel, such as lowering it when the weather is bad, reduces the problem of reflection from bubbles and is therefore recommended.

Validity of noise-extraction procedure during active pinging, E5

The result of the measurement series E5 for 18 kHz from a typical fish abundance estimation survey in the Barents Sea is shown in Figure 6. The weather conditions were good with sea state 2 and wind at 5–9 knots. Data were recorded first over 10 nautical miles with

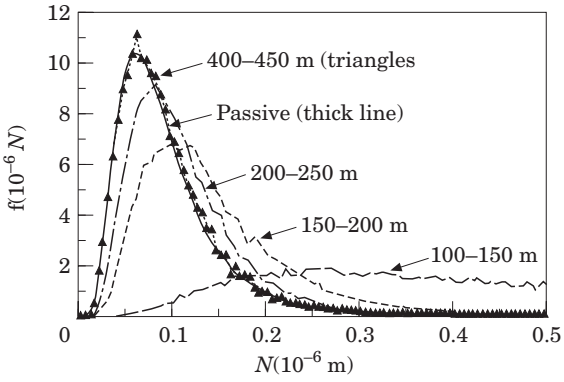

Figure 6. Quantification of noise from active data collected at survey conditions with the ship cruising at 11 knots in calm weather with about 450 m bottom depth. Data in the 400–450 m depth channel matches the purely passive data recordings almost exactly, but even the 200–250 m depth channel is close.

active transmission of sound, then with the echo sounder operated in passive mode for 5 nautical miles for comparison. The bottom was relatively flat with a depth of about 450 m. The experimental probability density function "f" from the passive recordings is plotted as a thick curve. Data from the active recordings are collected in depth channels paralleled to the bottom, each channel of 50 m thickness. The experimental probability density function from each of the depth channels is plotted.

At 18 kHz the "ringing" or extinction of echoes from the bottom is not complete until about 400 m below bottom with data being received more than 0.55 sec after the detected bottom; the match between the active and passive recordings is almost perfect in this case. However, even at 200 m there is a reasonable match between the relative frequency densities of the active and passive data. Measurements for other frequencies shows similar results but the time or the depth below bottom for the noise to reach a stable level is obviously frequency dependent. The signal attenuation is probably also dependent on the shape and hardness of the bottom. For the frequencies in use, 18, 38, 120, and 200 kHz, the depths below bottom where mean noise power index Ave(N) reached a stable value were 200, 120, 60 and 40 m respectively. Below these depths the measured signal is approximately the same as if the echo sounder were operated in passive mode.

In some echograms both first and second bottom echoes are recorded but comparison with passive recordings show that data below the second bottom echo should not be used. This is explained by increased noise below the second bottom echo caused by additional bottom–surface–bottom backscattering. For bottom depths less than 200 m, noise has to be calculated from data above bottom for 18 kHz. For extremely dense concentrations of fish where the calculation fails, noise from one of the previous pings has to be used. An alternative is to use the expected noise variation due to bottom depth as a criteria for switching to passive data recording for a few seconds, especially if this could be done automatically by the echo sounder. In general, however, the effect of noise correction is small both for 18 and 38 kHz, at least down to 750 m, and is therefore necessary only when the noise is known to be large. Noise at 18 kHz may be reduced by using a more directive transducer or a higher sampling rate, but this frequency will still be subject to external noise as compared to the other frequencies.

Application of the noise-reduction method

The effect of noise correction is great at 200 kHz and allows targets hidden in the noise as deep as 450 m from the transducer to emerge. The effect of noise correction on a one nautical-mile echogram at 200 kHz is shown in Figure 7. Note the change in area backscattering coefficients s_A and in the visual impression. Close to the bottom in the noise-corrected echogram can be seen structures invisible in the original echogram.

For the extremely densely distributed wintering herring schools in Ofotfjorden, 200 kHz data can be used with care for density measurements at least down to 300 m and perhaps down to 350 m, based on comparisons with 38 kHz data. For smaller targets, the range limits the effective sampling volume according to Ona (1987) and Foote (1991). Noise correction at both 120 and 200 kHz are necessary if these frequencies are to be used in combination with 38 and 18 kHz.

There are also other applications of continuous noise measurements: measurements of persistent noise can be used as a general noise threshold value for example, and the change in persistent noise, with the same vessel speed and keel depth, is an indication of instrument problems for the highest frequencies. Measurements of bottom-reflected propeller noise can to some extent also be used to check propeller damages. A silent propeller has been demonstrated to be an imperative during surveys for pelagic fish (Olsen *et al.*, 1982).

Implications of the experiments

Even if the recorded noise is corrected as proposed, the strength of the reflected propeller noise raises the question of fish avoidance from the vessel, which results in the underestimation of the fish density. Propeller noise backscattered from not very dense schools is easily detected, as shown in Figure 5. The radiated energy from the propeller is, of course, apparent even if not reflected. In bad weather, when bubbles generate noise and when propeller noise may be backscattered by bubbles, the echo sounder will experience higher levels

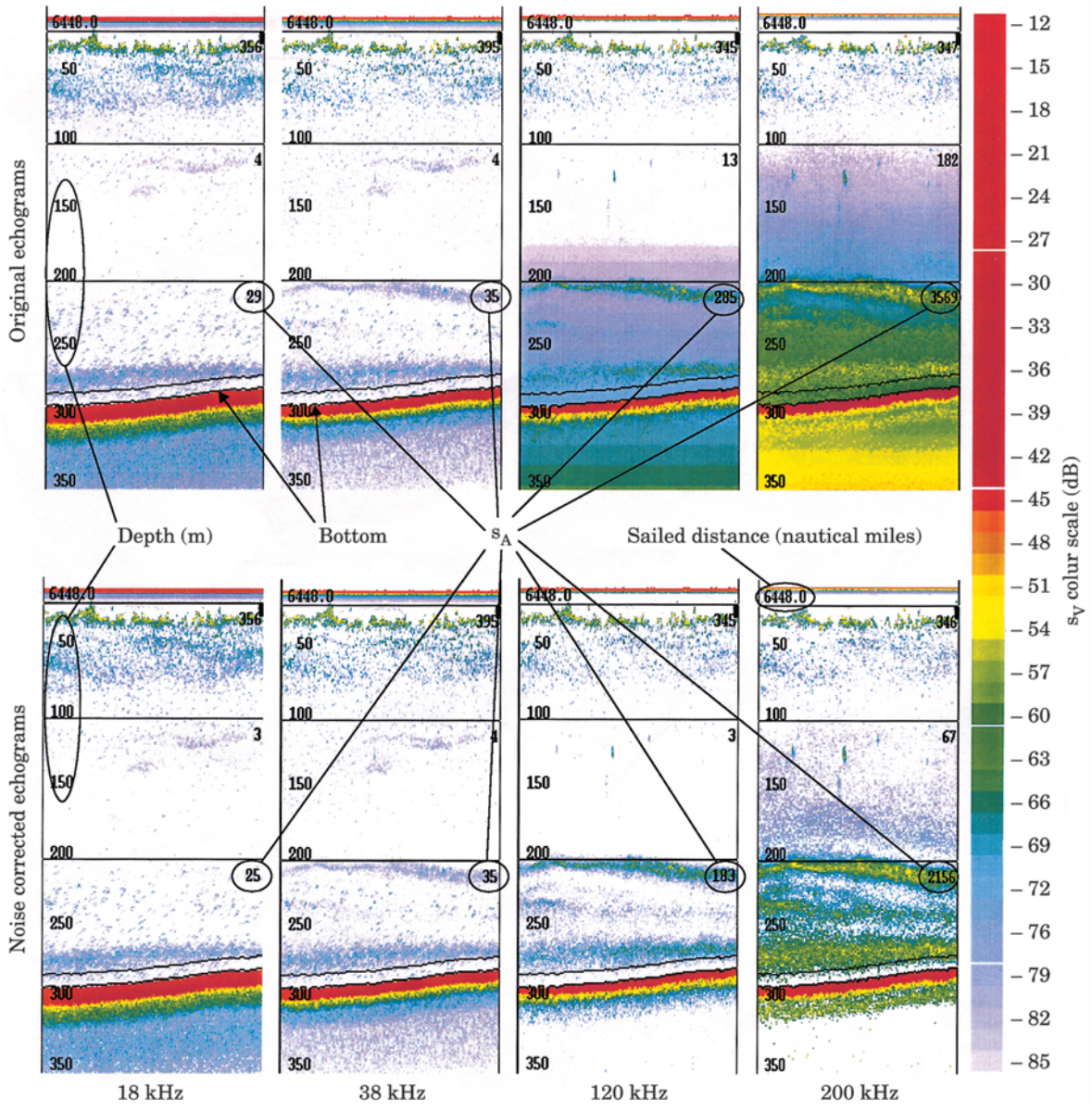

Figure 7. Example of noise correction according to equation (8) for 1 nmi echogram. For each frequency, the same value of N_E and $N_{H,10}$ are used for all of the echogram, since noise did not change significantly throughout the echogram because of stable weather conditions, vessel speed and bottom depth. The circles marks the original s_A (where s_V are used instead of $s_{V,S}$) and after noise removal. The values of N_E and $N_{H,10}$ in units of $(nmi^{-2}\ m^{-1})$ are 1.0×10^{-6} and 3.0×10^{-6} at 18 kHz, 0.045×10^{-6} and 0.15×10^{-6} at 38 kHz, 0.45×10^{-6} and 0.48×10^{-6} at 120 kHz, and 1.25×10^{-6} and 1.5×10^{-6} at 200 kHz.

of noise than in bad weather, but on the other hand, the fish would probably not react as much to the passage of the ship. With respect to the construction of new research vessels it is therefore important to reduce the propeller noise, and, by using the quietest possible engine coupled to the propeller, to reduce noise radiation and hence, presumably, vessel avoidance. This will also increase the effective detection and operating range of the echo sounders and SONARs used.

Summary

The method proposed for noise extraction and removal is applicable at all frequencies and is capable of both showing rapid variations in noise and correcting or removing them from echo recordings. For active transmission only data received some time after the first bottom echo and before the second should be used to calculate noise.

As expected and confirmed by experiments E3 and E4, the EK500/18 kHz system is more exposed to noise from external sources than at higher frequencies. The EK500/38 kHz system is exposed to external noise sources, but not as much as that at 18 kHz, and it is less affected by instrument noise than at 120 and 200 kHz. Instrument noise dominates at 200 kHz and, especially, 120 kHz.

The level of persistent noise is found from experiment E1, and the results from experiment E2 show that inter-frequency interference can be ignored except for 38 kHz in combination with an active 18 kHz system. Experiment E3 shows that noise is dependent on keel depth. Based on the results of experiment E3, the protruding keel was kept at the same depth throughout the measurements in experiment E4. The effect of persistent noise is removed from the measurement in experiment E4. The result is varying noise with the propeller as the main source. Some measurements of wind-induced noise show surprisingly little dependency on the wind when the protruding keel is at its maximum depth. The method of noise extraction from active transmission of sound is validated against passive data in experiment E5.

Acknowledgements

The Norwegian Research Council is thanked for financial support through grant 113517/122. Kenneth Foote is thanked particularly for reviewing the manuscript, especially for his help in simplifying the model. Professor Halvor Hobæk and Egil Ona are thanked for helpful comments on the manuscript.

Appendix

Essential symbols and definitions

g(t) (m^2)	Range-dependent amplification for area backscattering, also called 20log(r) Time Varied Gain (TGV), where $G(t)=r^2 10^{\alpha r/5000}$, r=ct/2 (m) is range from transducer surface to target, t(s) is time, c (m s^{-1}) is sound speed, α (dB km^{-1}) is absorption.
C	Constant including amplification and calibration constant.
U (V)	Voltage between transducer terminals, as well as transducer noise.
U_S	Signal part of U, i.e. transformed backscattered pressure only.
U_N	Noise part of U, i.e. transformed noise pressure and transducer noise, as well as instrument noise.
s_V (m^2 nmi^{-2} m^{-1})	Volume backscattering coefficient. $s_V=4\pi 1852^2 s_V$. See e.g. Medwin and Clay (1998) for definition of s_V. nmi=nautical mile. Here, one nautical mile is always exactly 1852 m.
$s_{V,S}$	Signal part of s_V after removal of noise.
$s_{V,N}$	Noise part of s_V.
s_A (m^2 nmi^{-2})	Area backscattering coefficient, $s_A=\int_{r_1}^{r_2} s_V dr$. See e.g. Foote and Knudsen (1994).
N (nmi^{-2} m^{-1})	Noise power index. Noise contribution to s_V is g(t)Ave(N) where Ave(N) is the sample. See Figure 2a for illustrations.
N_T	Value of $s_V/g(t)$ at the maximum of the experimental probability density function $f(s_V/g(t))$. Note that $N=s_{V,N}/g(t)=s_V/g(t)$ for the echosounder in passive mode (no sound transmission).
N_H	Maximum value of N used in calculations, $N_H>N_T$. $N_{H,10}$ is the value of N_H corresponding to $f(s_V/g(t))$ equal to 10% of $f(s_V/g(t))$ at maximum.
N_E	Average noise, only used in combination with active data. For passive data and for $N_H=N_{H,10}$ $N_E=Ave(s_V/g(t))$.
Y (−)	Normalized varying noise. Normalized average noise corrected for average persistent noise.
PSC (m^2)	Propeller source coefficient. $PSC=g(t)Y/10^6$. g(t) for range transducer-bottom-propeller.
Ping	Sound burst (pulse) transmitted from transducer.

References

Aglen, A. 1982. Echo integrator threshold and fish density distribution. FAO Fisheries Report, (300): 331 p, 33–44.

Foote, K. G. 1982. Optimizing copper spheres for precision calibration of hydro acoustic equipment. The Journal of the Acoustical Society of America, 71: 742–747.

Foote, K. G. 1991. Acoustical sampling volume. The Journal of the Acoustical Society of America, 90: 959–964.

Foote, K. G., Knudsen, H. P., Korneliussen, R. J., Nordbø, P. E., and Røang, K. 1991. Postprocessing system for echo sounder data. The Journal of the Acoustical Society of America, 90: 37–47.

Foote, K. G., Knudsen, H. P., Vestnes, G., MacLennan, D. N., and Simmonds, E. J. 1987. Calibration of acoustic instruments for fish density estimation: A practical guide. ICES Cooperative Research Report No. 144.

Foote, K G., and Knudsen, H. P. 1994. Physical measurement with modern echo integrators. The Journal of the Acoustical Society of Japan, 6(15): 393–395.

Hall, M. V. 1989. A comprehensive model of wind-generated bubbles in the ocean and predictions of the effects on sound propagation at frequencies up to 40 kHz. The Journal of the Acoustical Society of America, 86: 1103–1117.

Huse, I., Korneliussen, R. J. 1995. Diurnal variations in acoustic measurements of wintering Norwegian spring spawning herring. ICES CM 1995/B: 12, Ref. H (mimeo), 17 pp.

Korneliussen, R. 1993. Advances in Bergen Echo Integrator. ICES CM 1993/B: 28 (memeo).

MacLennan, D. N. 1990. Acoustical measurement of fish abundance. The Journal of the Acoustical Society of America, 87: 1–15.

Medwin, H., and Clay, C. 1998. Fundamentals of Acoustical Oceanography. Academic Press, New York.

Mitson, R. B. 1995. Underwater noise of research vessels. ICES Cooperative Research Report, No. 209.

Nunnallee, E. P. 1987. An Alternative Method of Thresholding during Echo Integration Data Collection. International Symposium on Fisheries Acoustics, June 22–26, 1987, Seattle, Washington, USA, 12 pp.

Ona, E. 1987. The equivalent beam angle and its effective value when applying an integrator threshold. ICES CM 1987/B: 35 (mimeo).

Ona, E., and Traynor, J. 1990. Hull mounted protruding transducer for improved echo integration in bad weather. ICES CM 1990/B: 3: 1–10.

Olsen, K., Angell, J., and Pettersen, F. 1982. Observed fish reactions to a surveying vessel with special reference to herring, cod capelin and polar cod. *In* Symposium on Fisheries Acoustics. Ed. by O. Nakken, and S. C. Venema. Bergen, Norway.

SIMRAD EK500 Scientific echo sounder. Instruction manual. P2172E, 1990–1997. Contents: Operators manual, P2170E Installation Manual P2180E, Service Manual 2161E.

Takao, Y., and Furusawa, M. 1995. Noise measurement by echo integrator. Fisheries Science, 61: 637–640.

Urick, R. J. 1983. Principles of Underwater Sound. Third edition. McGraw-Hill, New York.

Watkins, J. L., and Brierly, A. S. 1996. A post-processing technique to remove background noise from echo-integration data. ICES Journal of Marine Science, 53: 339–344.